THE JOURNAL OF PHYSICAL CHEMISTRY C

Article

pubs.acs.org/JPCC

Using Gibbs Energies to Calculate the Pt(111) H_{upd} Cyclic Voltammogram

Haleema Aied Asiri and Alfred B. Anderson*

Chemistry Department, Case Western Reserve University, Cleveland Ohio 44106-7078, United States

ABSTRACT: The cyclic voltammogram for hydrogen on Pt(111) has been calculated using potential-dependent Gibbs reduction energies obtained by the Interface 1.0 code. The reversible potentials, U_{rev}, are predicted by the equilibrium condition where the Gibbs energy of the oxidized reactant plus an electron and the Gibbs energy of the reduced product, when graphed as functions of electrode potential, cross and are equal at the reversible potential. Reversible potentials are calculated for 12 different coverages of H(ads), and a third-order analytic function is fit to the results. Using the derivative of this function, the experimental voltage scan rate, and the experimentally observed maximum H(ads) coverage, the cyclic voltammogram can be calculated. With the Langmuir isotherm contribution $-T\Delta S$ added to the Gibbs energies, the width of the predicted voltammogram and its maximum current density compare favorably with measurements from the literature. In detailed shape, the predicted current densities are curved more than the experimental ones near the maximum values, which is a feature ensured by the addition of the Langmuir term, which has an inflection at 0.5 ML coverage. This suggests the need for modification of the Langmuir isotherm near 0.5 ML coverage and possibly subtle improvements to the surface models used.

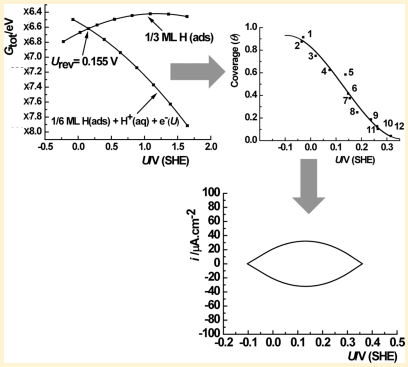

1. INTRODUCTION

Standard reversible potentials, U^0, are those potentials which apply to reduction reactions where reactants and products are in their standard states. These potentials are related to the standard reaction Gibbs energy, $\Delta_{react}G^0$:

$$U^0 = -\Delta_{react}G^0/(nF) \quad (1)$$

In this equation n is the number of electrons transferred and F is the Faraday constant. If U^0 is not easily measured electrochemically, it may be determined using eq 1 when $\Delta_{react}G^0$ is known by means of thermodynamic data found by experiment or theory.

Electrodes in a cell generally are not totally inert when participating in electron transfer reactions. The single crystal Pt(111) electrode in a standard hydrogen half-cell reduces some $H^+(aq)$ as the potential is swept from the 0.6−0.4 V double layer region toward 0.0 V reversible hydrogen half-cell potential. The reduction on the 0.4−0.0 V region deposits H(ads) on the electrode surface, which is usually called underpotential deposited hydrogen, or H_{upd}. When, during the sweep, 0.0 V is reached, the reduction forms hydrogen gas:

$$H^+(aq) + e^- = {}^1/_2H_2(g) \quad (2)$$

Prior to reaching 0.0 V, if the potential is held at some value in the 0.4−0.0 V range, there will be an equilibrium surface coverage of H(ads). The coverage starts at 0.0 monolayers (ML) and increases as the potential is decreased toward 0.0 V. However, when the platinum electrode is immersed in uniform acid solution and H_2 is not bubbled over it, then, since H_2 in the ambient is at low pressure, the onset potential for H_2 formation is given approximately by the Nernst equation,

$$U = 0.0 - 0.059\log\{P(H_2)^{1/2}/[H^+]\} \quad (3)$$

and is greater than 0.0 V. Measured onset potentials are around 0.05 V.[1,2]

Voltammograms show current densities as functions of electrode potential when the scan rate is constant and for the (111), (100), and (110) surfaces; they are reversible at typical scan rates. In the following, the potentials are referred to the reversible equilibrium state and would correctly be labeled as U_{rev}, but the subscript will be dropped in most of what follows. By assuming that the total charge passed in a branch of a cyclic voltammogram is linearly proportional to the coverage of upd species, it is easily shown that the current density at potential U, i.e. U_{rev}, is

$$i(U) = \pm KQ_{max}\, d\theta(U)/dU \quad (4)$$

where K is the constant scan rate in millivolts per second, Q_{max} is the maximum coverage achievable, and $d\theta(U)/dU$ is the slope of coverage with electrode potential. The + and − signs correspond to the oxidation and reduction waves, respectively. The challenge to applying eq 4 is calculating the dependence of H(ads) coverage on electrode potential. The purpose of this paper is to apply a self-consistent theory for the electrochemical interface, using the code Interface 1.0, to calculate $d\theta(U)/dU$ and predict the $i(U)$ voltammogram for the Pt(111) electrode. The (111) surface of platinum presents the simplest cyclic voltammogram in the upd potential region, with a broad hump in the oxidation and reduction potential directions, which

Received: February 23, 2013
Revised: June 7, 2013
Published: July 29, 2013

   dx.doi.org/10.1021/jp401909n | J. Phys. Chem. C 2013, 117, 17509−17513

means that the $d\theta(U)/dU$ factor in eq 4 approaches zero at the onset potential for upd hydrogen and as maximum coverage is reached, but is nearly constant over the broad hump range, and there is no contribution from $H_2O(l)$ oxidation to OH(ads). Voltammograms for the (100) and (110) surfaces are complex, with multiple peaks,[1,2] which means that there is more coverage-dependent variability in the slopes of $d\theta(U)/dU$ for these surfaces, and there are contributions from water oxidation to form OH(ads) in the H_{upd} potential ranges for the (100) and (110) surfaces.

2. COMPUTATIONAL APPROACH

The interface code[3,4] was used. This is a program for density functional calculations that employs atomic orbitals and atomic pseudopotentials. As in past studies with Interface, we used the RPBE functional.[5] In this work the two-dimensional band option was employed with adsorbates and electrolyte on one side of a three-atom thick slab of platinum atoms representing the electrode and vacuum on the other side. In two-dimensional density functional theory, the potential of the model electrode on the standard hydrogen electrode scale is easily evaluated as

$$U = -(E_f + \varphi)/e \quad (5)$$

where E_f is the calculated Fermi level energy, φ is the calculated work function of the standard hydrogen electrode, determined to be 4.43 eV in the interface calculation, and e is the electron charge unit. The potential is changed by adding or subtracting electronic charge on the translational unit cell. The counter charge is in a polarized electrolyte composed of 1.0 M 3.0 Å diameter positive and negative spherical charges and their density distribution is optimized using a modified Poisson–Boltzmann theory. The electrolyte also contains the dielectric continuum, which is a model for the implicit inclusion of bulk water. Water molecules that bond strongly with adsorbed or solution phase species by hydrogen-bonding or lone-pair donation are added to the calculations and the dielectric continuum is maintained in the model when this is done. Complete details are in refs 3 and 4.

We used a three-Pt layer slab with the bottom layer (on the vacuum side) atoms held rigidly in the calculated bulk structure with lattice constant 4.03 Å.[4] Positions of the platinum atoms in the central layer and the top layer (on the solution side) were variationally optimized in all calculations. Studied hydrogen atom coverage spanned from 1/12 monolayer (ML) to greater than 1.0 ML.

It is necessary to establish the surface adsorption site for upd H for our theoretical study. From the experimental side, in 1994 Ogasawara and Ito found evidence by in situ infrared reflection adsorption spectroscopy that at the electrochemical interface upd hydrogen is on terminal sites atop a single Pt atom on the (100) and (110) surfaces, but on the (111) surface terminal, bonded H was not seen.[6] However, shortly thereafter a sum-frequency generation determination of vibrational spectra of H at the electrochemical interface by Tadjeddine and Peremans gave evidence that in the upd potential range H is adsorbed on the atop site.[7] It is still uncertain which structure for upd H on Pt(111) is correct, and for a recent discussion of this and the overall issue of upd hydrogen, the reader is referred to the review of Jerkiewicz.[8]

The structure results for upd H on Pt(111) are also mixed from the theoretical side. In the case of the vacuum interface, different computational methods seem to agree that the differences in energies between 3-fold fcc, 3-fold hcp, 2-fold bridging, and 1-fold atop sites are small.[9] In the literature,[9] some DFT slab-band calculations for Pt(111) found the atop site to be most stable, some the fcc site, and one favored the bridge site. Some of these calculations showed stronger adsorption at the higher of two coverage models studied, which implies such models will not be able to account for the smooth cyclic voltammograms in the upd H potential range on Pt(111). This is because the interaction parameter of the Frumkin isotherm is positive,[1] and further analysis in ref 1 yielded the coverage dependence of the adsorption enthalpy, which showed interactions between adsorbed H to be repulsive.

Calculations for the electrochemical interface including the double layer are small in number. Hamada and Morikawa developed a model to calculate the potential dependence of the Pt–H vibrational frequency.[10] In their DFT slab-band calculations, they included variable electric fields, variable degrees of H(ads) coverage, and variable amounts of explicit water molecules. With just the field added, the fcc site was favored for different coverage models. But, with water molecules added, structures were found in which the 1-fold atop site was the most stable adsorption site for H.

An earlier computational approach to predicting the cyclic voltammogram from adsorption energies is that of Norskov and co-workers who added ad hoc contributions to a DFT slab-band vacuum interface model to calculate H adsorption Gibbs energies.[11] In their model, H(ads) was placed in the fcc site favored by vacuum interface calculations and the thermal and entropy terms added to the calculated adsorption internal energies were estimated using calculated vibrational energy levels. Adsorption Gibbs energies were obtained for different degrees of coverage, all at the potential of zero charge, meaning the effect of electrode charging on the strength of the PtH bonds was nil in the model. No double layer or field was employed, and the potential dependence was taken to be linear in the calculated Gibbs adsorption energy of $^1/_2H_2(g)$, $\Delta G = \Delta G^0 + eU$, with the value of zero when $\Delta G = \Delta G^0 = 0.0$. In their model, the adsorption Gibbs energies were calculated to decrease linearly with increasing coverage of H(ads) up to 1.0 ML, showing Frumkin behavior. They added a Langmuir isotherm contribution due to configurational entropy to the Gibbs energy:

$$-T\Delta S_{conf}(\theta) = -Tk_b \ln[(1-\theta)/\theta] \quad (6)$$

Using this and the calculated $U(\theta)$ data, they determined $d\theta(U)/dU$ for use in eq 4 and thereby obtained qualitative fits to an experimental cyclic voltammogram for upd H on Pt(111).

3. RESULTS AND DISCUSSION

In this study, we have used Interface to calculate Gibbs adsorption energies for H as functions of its coverage on Pt(111) at 298.15 K. Gibbs and internal energies for H(ads) on the 1-fold atop site were more stable than the fcc site over the potential range studied. We used 11 different coverage models, with 10 of the structures shown in Figure 1. The translational cells are outlined in the figure, and the number of atoms used is shown. For the 1/12 ML coverage shown, a 36 Pt atom translation cell was required, and for 1/6, 1/3, 1/2, 2/3, 5/6 and 1 ML, an 18 Pt atom cell was used. This sequence was employed to generate coverage-dependent potentials over increments of 1/12 and 1/6 ML. For the 1/8 ML coverage shown, a 24 Pt atom cell was required, and for the 1/4, 1/2, 3/4, and 1 ML sequence, a 12 Pt atom cell was used.

dx.doi.org/10.1021/jp401909n | J. Phys. Chem. C 2013, 117, 17509–17513

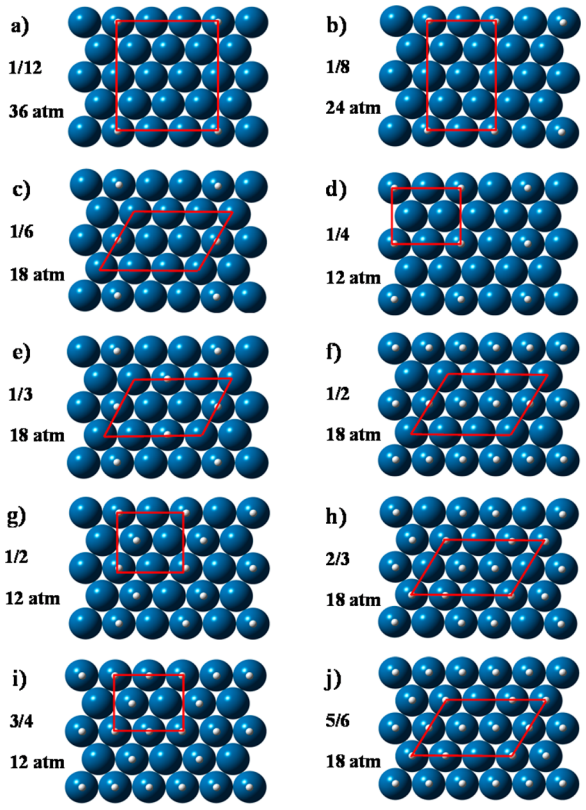

Figure 1. Top view of various structures of H adsorption on Pt (111) surface arranged from low to high coverage (ML) and labeled a–j. Translational cells and number of atoms are shown for all but 1.0 ML coverage.

We employed the dielectric continuum model and the modified Poisson–Boltzmann theory without explicit water molecules. Water molecules interacted weakly with adsorbed H atoms and surface platinum atoms. This is a case where the dielectric continuum model is adequate, and including them and optimizing their structures would have greatly increased computation times.

The reversible potentials for incremental increases in H(ads) coverage were calculated as the crossing points for the Gibbs energies of reactants and products, as shown for a typical example in Figure 2. In this case, the coverage changes between 1/6 and 1/3 ML. The resulting reversible potential was assigned to the average H(ads) coverage used in its determination. Interestingly, the G versus U curves in this

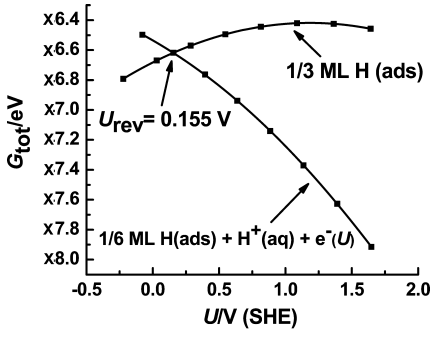

Figure 2. At reversible potentials, U_{rev}, reactant and product Gibbs energies are equal.

and the other figures (not shown) are well fit by second-order polynomials and the vertical distances between the curves, $G_{ox}(U) - G_{red}(U)$, are nearly linear in $U - U_{rev}$. This is the consequence of the functions $[G_{ox}(U) - U]$ being only a little perturbed in shape when small additional amounts of H(ads) are deposited on or removed from the surface. Table 1 shows

Table 1. Calculated Reversible Potentials, U_{rev}, Using the Method of Figure 2

U_{rev}	θ_{oxd}	θ_{red}	patterns
0.032	5/6	1	*j*, 1
0.048	2/3	5/6	*h*, *j*
0.146	1/2	2/3	*f*, *h*
0.139	1/3	1/2	*e*, *f*
0.155	1/6	1/3	*c*, *e*
0.212	1/12	1/6	*a*, *c*
0.015	3/4	1	*i*, 1
0.088	1/2	3/4	*g*, *i*
0.141	1/4	1/2	*d*, *g*
0.200	1/8	1/4	*b*, *d*
0.209	0	1/8	0, *b*
0.235	0	1/12	0, *a*

[a] θ_{oxd} and θ_{red} are the initial and final H coverages in the patterns keyed to Figure 1.

the calculated reversible potentials and the coverage pairs and structure patterns used in calculating them. All of the resulting potentials are plotted as a function of coverage in Figure 3, but

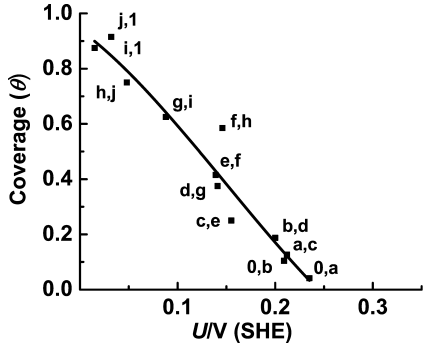

Figure 3. Calculated H coverage vs Pt(111) electrode potential excluding Langmuirian configurational entropy contribution, based on data in Table 1.

with U and $\theta(U)$ as the ordinate to make it easy to visualize the slope $d\theta(U)/dU$ for use in eq 4. A third-order polynomial curve is fit to the data so that the derivative can be determined analytically from the fit. It is seen that over the potential range 0–0.25 V, the coverage goes from 0.0 ML to an upper limit of about 0.9 ML.

Some points in Figure 3 are further from the third-order fitting than others. At this time no rationalization for these deviations is evident. As examination of Figure 1 will show, the adsorption patterns chosen for each coverage are constrained by the sizes of the translational cells used and so are not well randomized. It is expected that by the use of very large translational cells and resulting energies for a given coverage a more random most stable pattern would be found. One step further in accuracy could be to use a Boltzmann distribution at the ambient temperature over many such patterns. In the high and low coverage limits the potentials may be more accurate

dx.doi.org/10.1021/jp401909n | J. Phys. Chem. C 2013, 117, 17509–17513

because the sparse H(ads) and H(ads) vacancies are well separated. Finally, weak interactions of water molecules may exert subtle influences.

The potential span of Figure 3 is too narrow to produce the experimental upd H voltammograms in which H appears on the surface at about 0.4 V during a negative voltametric sweep from the double layer potential region, and the last remnant departs at about 0.4 V during the oxidation sweep. For each point of the θ versus U curve in Figure 2, we may write

$$\Delta G(\theta) = -FU(\theta) \quad (7)$$

Adding the configutational entropy contribution to the Gibbs energy, eq 6, gives a new equation for potential,

$$U(\theta) = -\Delta G(\theta)/F + [Tk_b/F]\ln[(1-\theta)/\theta] \quad (8)$$

The Langmurian contribution broadens the coverage versus potential curve so that it takes the new form in Figure 4, with the two highest coverage points shifted to negative potentials. Table 2 contains the data plotted in Figures 3−5.

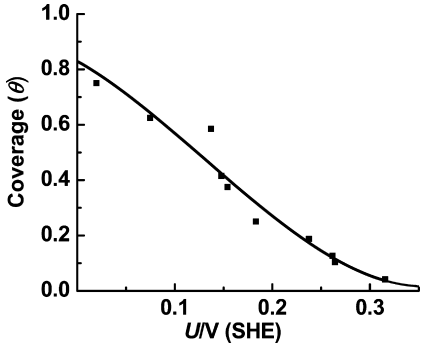

Figure 4. Calculated H coverage vs Pt(111) electrode potential including Langmuirian configurational entropy contribution.

Table 2. Values of H(ads) coverage used in Figures 3−5 and Corresponding Reversible Potential Energies for Reduction from Interface Calculations and with $T\Delta S_{conf}$ Included

coverage (θ)	U_{rev}	point	$U_{rev} - RT\Delta S_{conf}/F$
0.917	0.032	1	−0.029
0.750	0.048	2	0.0198
0.583	0.146	3	0.1378
0.417	0.139	4	0.148
0.25	0.155	5	0.183
0.125	0.212	6	0.262
0.875	0.015	7	−0.035
0.625	0.088	8	0.0749
0.375	0.141	9	0.1549
0.188	0.200	10	0.238
0.062	0.209	11	0.2648
0.042	0.235	12	0.316

In Figure 5 the fitted curve extends to the region of zero slope, about −0.1 V. This curve is converted into a cyclic voltammogram by evaluating $d\theta(U)/dU$ as the derivative of the analytic third-order fitting curve and multiplying by the 50 mV s^{-1} scan rate, and by Q_{max} = 210 μC cm^{-2}. The predicted voltammogram is in Figure 6. For full monolayer coverage of Pt(111), Q_{max} would be 240 μC cm^{-2}, but in their combined cyclic voltammetric and chronoamperometric study Strmcnik et al. measured the lower value.[2] They were able to do this by

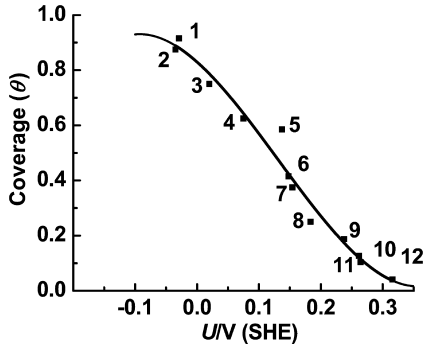

Figure 5. Calculated H coverage vs Pt(111) electrode potential including Langmuirian configurational entropy contribution and extended to negative potentials. Data points are numbered in connection with Table 2.

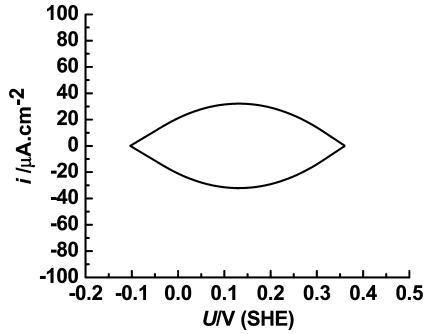

Figure 6. Predicted cyclic voltammogram at 298.15 K.

measuring the H adsorption isotherm to about −0.1 V. Their reconstructed cyclic voltammogram extended down to −0.1 V and at 0.05 V, where H evolution commences, the surface coverage was only about 2/3 ML. Our calculated coverage at 0.05 V, taken from Figure 5, is 0.72 ML, in close agreement. Our calculated maximum coverage is 0.91 ML, taken from Figure 5, is in close agreement with 210/240 = 0.875 ML as estimated by Strmcnik et al. The maximum current density we calculate, taken from Figure 6, is 32 μA cm^{-2}, which is between the values 27 μA cm^{-2} which we estimate from Figure 2b in the paper by Strmcnik et al. and 34 μA cm^{-2} which we estimate from Figure 1 in the paper by Gomez et al.[1] To illustrate the agreement between our predicted voltammogram and the one in Figure 2b by Strmcnik et al., we have superimposed the two in Figure 7. The authors did not specify the temperature of the measurements, which was presumably close to 298 K. Gomez et al. illustrated the dependence of voltammogram shape on temperature in their Figure 1, where it may be seen that going up to 25 C higher or lower than ambient makes small graphical changes, but those changes do allow the determination of thermodynamic adsorption entropy and energies. Therefor it is concluded that the agreement with regard to width and height between the predicted voltammogram and the measured ones in refs 1 and 2 will not be graphically affected by changes in temperature of this magnitude.

The Norskov group results in ref 11 overestimated the maximum current density, prediction it to be around 50 μA cm^{-2}. We have identified two contributing factors. One is they used monolayer coverage, for Q_{max}, corresponding to 240 μC cm^{-2}, in eq 4. When the measured value of Strmcnik et al., 210 μC cm^{-2}, is used, the maximum is reduced to about 44 μA cm^{-2}, still too high. The second factor is the calculated slope for

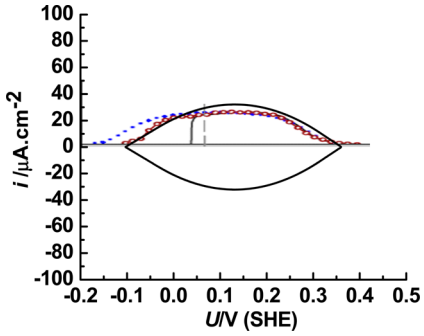

Figure 7. Superposition of voltammogram copied from Figure 2b in ref 2 on the predicted result in Figure 6. The red points are the extended voltammogram obtained from chronoamperometric experiments. The vertical gray line reaches zero current density at the experimental onset potential for hydrogen evolution. The blue dots are a theoretical projection in ref 2 based on a total coverage corresponding to 240 μC cm^{-2} total charge or 1.0 ML H(ads) final coverage.

use in eq 4, $d\theta(U)/dU$, which is too high. This factor causes the predicted width of the voltammogram wave to be too small, with current density approaching zero at about 0.30 V instead of 0.35 V as shown in Figure 7. Another difference is we find that the slope is not strictly constant as assumed in that work, but decreases in the high and low coverage limits, as may be seen in Figure 3.

Concluding Comments. Calculated reversible potentials for a limited sampling of surface coverage and adsorption patterns for H(ads) in Pt(111) can parametrize eq 4 to predict the voltammogram as shown here and also in the somewhat less accurate result reported in ref 11, where a simpler model for calculating Gibbs energies was used. There is need for improvement in the broad region of high current density where the predicted current density is not constant enough. This rather slight disagreement is due to the noticeable inflection in the middle of the calculated coverage versus potential graphs, much of which is a consequence of adding the Langmuirian $-T\Delta S_{conf}$ contribution to the Gibbs energy. For better agreement with experiment, the curves need to be closer to linear in this region, meaning the change in potential should be linear in changes in coverage. At this time we do not know what it is about the experimental system that achieves such linearity, whether the formula for the $-T\Delta S_{conf}$ contribution needs to be modified to apply only at high and low coverage, or if there is another explanation.

The Pt(100) and (110) surfaces present H_{upd} voltammograms with interestingly greater complexity. One difference from the (111) case is the interference of OH(ads) formation currents from the oxidation of $H_2O(l)$ with the H(ads) currents.[1,12] This was not an issue for the Pt(111) surface studied here, but for the other two surfaces, the higher potential regions where H(ads) is deposited have enhanced current density in the voltammograms. On the (100) surface there is a dip in current density at around 0.2 V.[1,2] In this region, $d\theta(U)/dU$ must decrease to zero. Around 0.4 V there is a two-peaked hump about 0.2 V wide which is broadened slightly by OH(ads) formation currents. On the Pt(110) surface there are two sharp peaks. Sharp peaks suggest rearrangement of H(ads) to new adsorption patterns when certain coverage is achieved as the potential cycles, that is, they suggest phase transitions. Such transitions would be caused by potential-dependent adsorption internal energies (bond strengths) and reorganizational entropies of the hydrogenated surface and of the double layer water molecules. A complete understanding has not yet been achieved. For further discussion the reader is referred to the cited literature.[1,2,8,12]

AUTHOR INFORMATION

Corresponding Author

*E-mail: aba@po.cwru.edu. Phone: 216-368-5044. Fax: 216-368-3006.

Notes

The authors declare no competing financial interest.

ACKNOWLEDGMENTS

H.A.A. gratefully acknowledges generous fellowship support from the Saudi Arabian Cultural Mission, and she expresses her appreciation to Dr. Ryosuke Jinnouchi for assistance with setting up the Interface code on the Case cluster. Preparation of the manuscript was aided by support from the National Science Foundation under Grant No. CHE-0809209.

REFERENCES

(1) Gomez, R.; Orts, J. M.; Alverez-Ruiz, B.; Feliu, J. M. Effect of temperature on hydrogen adsorption on Pt(111), Pt(110), and Pt(100) electrodes in 0.1 M $HCLO_4$. *J. Phys. Chem. B* **2004**, *108*, 228−238.

(2) Strmcnik, D.; Tripkovic, D.; van der Vliet, D.; Stamenkovic, V.; Markovic, N. M. Adsorption of hydrogen of Pt(111) and Pt(100) surfaces and its role in the HOR. *Electrochem. Commun.* **2008**, *10*, 1602−1605.

(3) Jinnouchi, R.; Anderson, A. B. Aqueous and surface redox potentials from self-consistently determined Gibbs energies. *J. Phys. Chem. C* **2008**, *112*, 8747−8750.

(4) Jinnouchi, R.; Anderson, A. B. Electronic structure calculations of liquid-solid interfaces: Combination of density functional theory and modified Poisson-Boltzmann theory. *Phys. Rev. B* **2008**, *77*, 245417-1−18.

(5) Hammer, B.; Hansen, L. B.; Norskov, J. K. Improved adsorption energetics within density-functional theory using revised Perdew-Burke-Ernzerhof functionals. *Phys. Rev. B* **1999**, *59*, 7413−7421.

(6) Ogasawara, H.; Ito, M. Hydrogen adsorption on Pt(100), Pt(110), Pt(111), and Pt(11 11) electrode surfaces studied by in situ infrared reflection adsorption spectroscopy. *Chem. Phys. Lett.* **1994**, *221*, 213−218.

(7) Tadjeddine, A.; Peremans, A. Vibrational spectroscopy of the electrochemical interface by visible infrared sum frequency generation. *J. Electroanal. Chem.* **1996**, *409*, 115−121.

(8) Jerkiewicz, G. Electrocatalytic hydrogen adsorption and absorption. Part 1: under-potential deposition of hydrogen. *Electrocatal.* **2010**, *1*, 179−199.

(9) Fearon, J.; Watson, G. W. Hydrogen adsorption and diffusion on Pt(111) and PtSn(111). *J. Mater. Chem.* **2006**, *16*, 1989−1996 and references therein.

(10) Hamada, I.; Morikawa, Y. Density-functional analysis of hydrogen on Pt(111): electric field, solvent, and coverage effects. *J. Phys. Chem. C* **2008**, *112*, 10889−10898.

(11) Karlberg, G. S.; Jaramillo, T. F.; Skulason, E.; Rossmeisl, J.; Bligaard, T.; Norskov, J. K. Cyclic Voltammograms for H on Pt(111) and Pt(100) from first principles. *Phys. Rev. Lett.* **2007**, *99*, 126101−1−4.

(12) Garcia-Araez, N. Enthaplic and entropic effects on hydrogen and OH adsorption on Pt(111), Pt(100), and Pt(110) electrodes as evaluated by Gibbs thermodynamics. *J. Phys. Chem. C* **2011**, *115*, 501−510.